A thermally tunable terahertz metamaterial absorber*

ZHENG Wei (郑伟), **LI Wei** (李伟), **and CHANG Sheng-jiang** (常胜江)**
Institute of Modern Optics, Nankai University, Tianjin 300071, China

(Received 20 October 2014)

A thermally tunable terahertz metamaterial absorber (MA) with InSb embedded in a metal-dielectric-metal structure is proposed. The transmission and tuning properties of the proposed metamaterial absorber are analyzed for the temperature ranging from 160 K to 350 K. The simulated results show that the maximum absorption of the absorber is nearly 99.8% at a full-width at half-maximum (FWHM) of 38 GHz, and the absorption frequency can be dynamically tuned from 0.82 THz to 1.02 THz.

Document code: A **Article ID:** 1673-1905(2015)01-0018-4
DOI 10.1007/s11801-015-4193-0

Nowadays, the applications of metamaterials have been demonstrated in the range from radio frequencies to terahertz (THz) and near infrared frequencies[1-4]. In THz regime, the metamaterial absorber (MA) can be used as a functional detector or imager. A further application of MAs is in the field of perfect lenses[5] and invisibility cloaks[6]. Since the MA was firstly proposed, the design, fabrication and characterization of MAs have been investigated extensively[7-9]. Shen et al[10] reported a triple-band THz MA with three absorption peaks. Tao et al[11] presented a wide-angle absorber for transverse electric and transverse magnetic radiation with absorption of 96% at 1.6 THz. Padilla et al[12] demonstrated an electronically tunable liquid crystal MA with a frequency tunability of 4.6%, but the maximum absorption only reached 80%. To simultaneously realize the high absorption and tunable characteristics is still a challenge.

Traditional MAs are usually composed of metal and dielectric medium, but they can not be actively controlled by thermal, electrical and optical means. The introduction of semiconductor materials into metamaterial structures can solve the problem above. The functional material of InSb, which is very sensitive to temperature, was introduced into THz plasmonic crystal firstly by Fan et al[13,14] for realizing high tunability.

In this paper, we propose a thermally tunable MA, in which the semiconductor InSb is embedded for achieving large frequency tunability. Numerical simulation indicates that the maximum absorption of 99.8% at a full-width at half-maximum (FWHM) of 38 GHz can be realized, and the absorption frequency can be dynamically tuned from 0.82 THz to 1.02 THz. This excellent tuning characteristic makes the proposed MA be a promising candidate for many potential applications, particularly in sensing, imaging, energy harvesting and dynamic scene projectors.

Generally, the MA with three-layer structure usually comprises a microstructure metallic layer, a metal wire or plate layer, and a dielectric layer between them[4,10,11], and the thickness of each layer is significantly smaller than the wavelength. Similarly, our MA is composed of an electric ring resonator (ERR) layer on the top, a dielectric layer in the middle and a metallic plate layer on the bottom, as shown in Fig.1(a). The ERR unit cell consists of two standard split ring resonators with 200 nm-thick InSb embedded in the split gaps. The dimensions of the ERRs are optimized as L=40 μm, the line width W=6 μm, the split gaps G=5 μm and the lattice constant A=50 μm. Both the ERRs and the metallic plate are made of gold with the thickness of 200 nm and a conductivity of 4×10^7 S/m. Silica glass is used as the dielectric layer with a thickness of 7.2 μm and a dielectric constant of 3.75 to separate two metallic layers. The total structure is constructed on 500 μm-thick silicon substrate as shown in Fig.1(b).

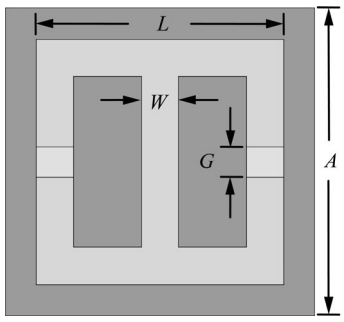

(a)

* This work has been supported by the National Basic Research Program of China (No.2014CB339800), the National High Technology Research and Development Program of China (No.2011AA010205), and the National Natural Science Foundation of China (Nos.61171027 and 10904076).
** E-mail: sjchang@nankai.edu.cn

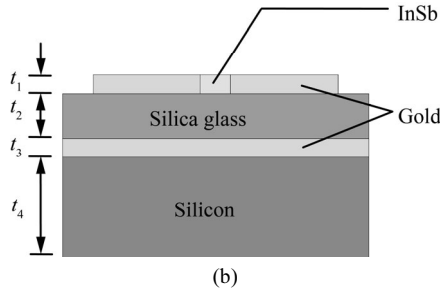

Fig.1 (a) The geometric structure and (b) the composition of a unit cell with optimized parameters of *L*=40 μm, *W*=6 μm, *G*=5 μm, *A*=50 μm, t_1=t_3=200 nm, t_2=7.2 μm and t_4=500 μm

In the THz regime, the electromagnetic properties of InSb are very sensitive to temperature. For temperatures ranging from 160 K to 350 K, the complex dielectric function of InSb can be approximately given by the Drude model as[15]

$$\varepsilon(\omega)=\varepsilon_{\infty}-\frac{\omega_{\mathrm{p}}^2}{\omega^2+\mathrm{i}\gamma\omega}, \tag{1}$$

where ε_∞ represents the high-frequency permittivity, ω is the angular frequency of incident THz wave, and γ is the damping constant. The plasma frequency $\omega_{\mathrm{p}}=\sqrt{Ne^2/\varepsilon_0 m^*}$ depends on the intrinsic carrier density N, the electronic charge e, the vacuum permittivity ε_∞ and the effective mass m^* of free carriers. For InSb, ε_∞=15.6, m^*=0.015m_{e} (m_{e} is the mass of electron), γ=0.1π THz[16], and the intrinsic carrier density N with unit of m^{-3} obeys the relationship[17]

$$N=5.76\times10^{20}T^{1.5}\exp\left(-0.26/2k_{\mathrm{B}}T\right), \tag{2}$$

where k_{B} is the Boltzmann constant, and T is the temperature in Kelvin. According to the above expressions and parameters, the complex permittivity of InSb can be calculated at various temperatures.

In general, the absorption frequency is dominantly determined by the ERR since it acts as a frequency selective surface. Fig.2(a) depicts the equivalent circuit of the MA, where LC and R determine the resonance frequency and the resistivity of metal in ERRs, respectively, and the arrows represent the direction of the induced currents. The variable capacitance C can be changed when the temperature of InSb embedded in the split gaps changes. In other words, the resonance frequency in ERRs depends on the change of temperature. Furthermore, the surface structure of ERRs can only reflect the incident THz waves partially. As shown in Fig.2(b), most of the incident THz waves traverse the ERRs into the dielectric layer, undergo multiple reflections and transmissions between the upper and lower interfaces, and eventually transmit through the ERRs with little absorption by the dielectric layer. Considering the above process, another LC circuit should be added in the model as seen in Fig.2(a), where $\mathrm{L_pC_p}$ determines the resonance frequencies inside dielectric layer, and $\mathrm{R_p}$ represents any loss in the absorber. In this model, changing permittivity of InSb can affect the values of LC and $\mathrm{L_pC_p}$ simultaneously. Whenever both resonant frequencies match, $\mathrm{R_p}$ will get short-circuited and the MA will theoretically achieve perfect absorption[18]. In this case, the currents of I and I_x have the same magnitude but are out of phase, so that they will cancel out each other in $\mathrm{R_p}$. As shown in Fig.2(b), we consider I as the reflected wave on ERRs layer and I_x as the transmitted wave through ERRs layer from inside dielectric layer, and then this model is consistent with the interference theory.

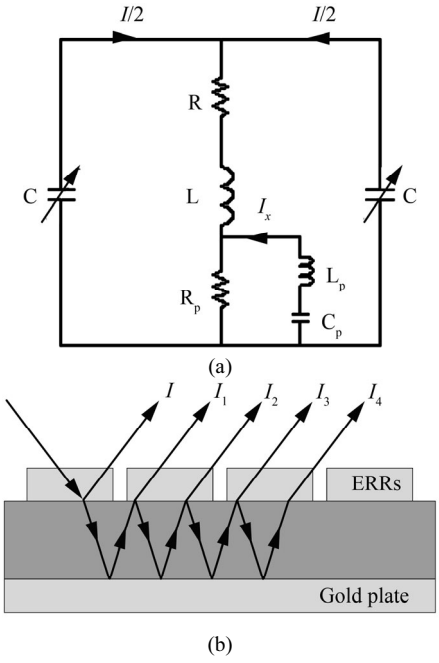

Fig.2 (a) The equivalent circuit of the MA; (b) The physical model to explain the absorption process

Utilizing the finite-difference time domain (FDTD) method, we calculate the absorption spectra at various temperatures, as shown in Fig.3(a). The incident THz wave is assumed to be normal to the upper surface of MA with the electric field perpendicular to the split gaps. The absorption coefficient A can be expressed as A=1–T–R, where T and R are transmission and reflection coefficients, respectively. Since the thickness of the gold plate on the bottom is much larger than its skin depth in THz range[19], the transmittance should be zero. Accordingly, the absorption coefficient can be simplified to A=1–R. At the low temperature of 160 K, the intrinsic carrier density of InSb is $N\approx0.94\times10^{20}$ m^{-3}, and InSb shows typical dielectric features. The maximum absorption of 88.7% locates at 0.82 THz with FWHM of 26 GHz. In the case of a non-perfect absorber, the LC and $\mathrm{L_pC_p}$ resonance frequencies are mismatched, which means that the phase difference between I and I_x is not equal to π, and the total reflected power is not zero. As the temperature is increased, the variable capacitance C is decreased due to the enhancement of intrinsic carrier density of InSb. At 290 K, the carrier density is $N\approx1.57\times10^{22}$ m^{-3}, and InSb shows typical metallic features. In this case, the absorption peak with a maximum absorption of 93.3% shifts to 0.90 THz, and the

LC value is so close to L_pC_p value that both resonance frequencies get matched due to the variable capacitance C decreases along with the temperature increasing to 320 K. The absorption peak shifts to 0.95 THz, and the maximum absorption and FWHM are 99.8% and 38 GHz, respectively. The carrier density N can reach 5.76×10^{22} m^{-3} along with the temperature increasing to 350 K, the LC resonance frequency will again stay away from L_pC_p resonance frequency, and then the maximum absorption of 90.3% is obtained at 1.02 THz with FWHM of 52 GHz. Actually, the thickness of the dielectric layer is also a very important parameter which can cause large changes in absorption spectrum. Fig.3(b) shows the absorption peak versus the thickness of the dielectric layer changing from 5 μm to 9 μm at different temperatures. For our MA, the optimal thickness of t_2 is 7–7.5 μm, and too large or too small thickness of the dielectric layer will lead to lower absorption due to mismatch of LC and L_pC_p resonance frequencies.

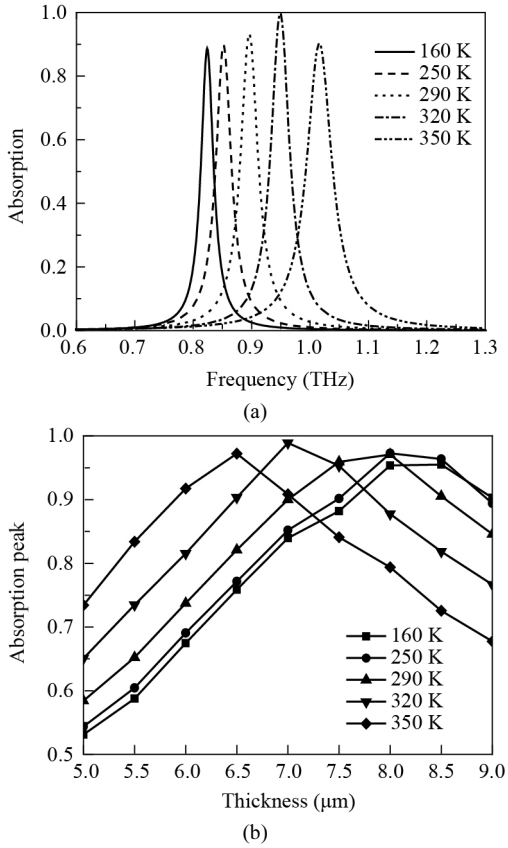

Fig.3 (a) Simulated absorption spectra of the MA at different temperatures with the FDTD method; (b) The absorption peak versus the thickness of the dielectric layer at different temperatures

For the temperature of 320 K, the electric energy distributions at 0.95 THz show the nearly perfect absorption characteristics inside the absorber, as seen in Fig.4. The majority of the energy is dissipated as ohmic loss in the ERRs layer and dielectric loss in the dielectric layer. The region of maximum absorption is located in the split gaps which are embedded by InSb. Additionally, the electric energy is also concentrated in the four outer corners of the ERR. It is clear that the original THz transmission mode of ERRs is changed by the metallic features of InSb at the high temperature of 320 K.

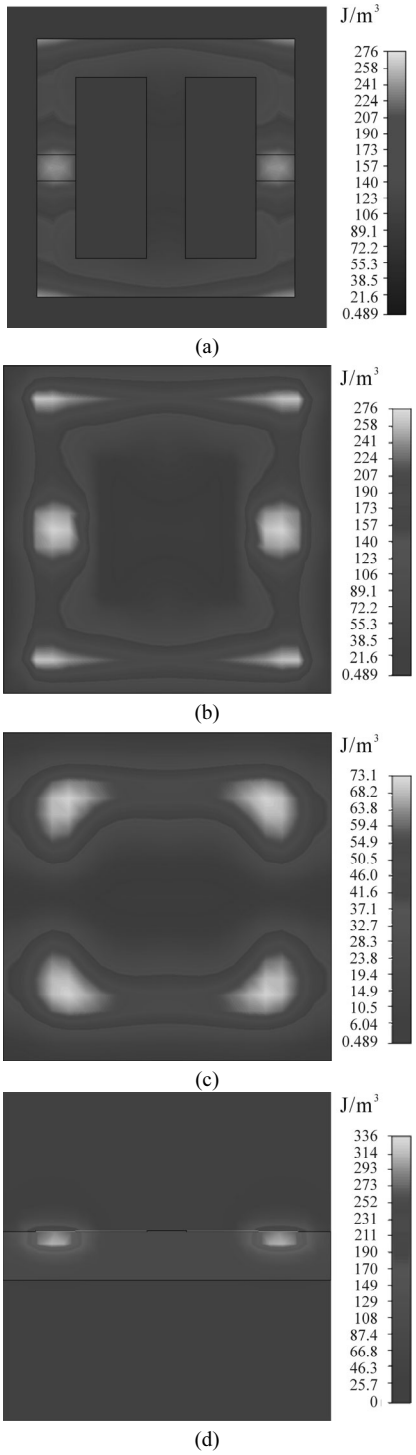

Fig.4 The electric energy distributions in (a) ERR layer, (b) dielectric layer, (c) metallic plate and (d) cross section along the split gaps at frequency of 0.95 THz and temperature of 320 K

In summary, we propose a thermally tunable THz MA.

Its maximun absorption is almost more than 90%, and the FWHM is less than 60 GHz. When the temperature changes from 160 K to 350 K, the absorption frequency can be dynamically tuned from 0.82 THz to 1.02 THz. Especially, when the temperature is 320 K, the MA has a nearly perfect absorption at the frequency 0.95 THz. As a narrow band device, the tunable MA will have a potential application in future THz system.

References

[1] WANG Chang-hui, KUANG Deng-feng, CHANG Sheng-jiang and LIN Lie, Optoelectronics Letters **9**, 266 (2013).

[2] LI Wei, CHANG Sheng-jiang, WANG Xiang-hui, LIN Lie and BAI Jin-jun, Optoelectronics Letters **10**, 180 (2014).

[3] C. Enkrich, M. Wegener, S. Linden, S. Burger, L. Zschiedrich, F. Schmidt, J. F. Zhou, Th. Koschny and C. M. Soukoulis, Physical Review Letters **95**, 203901 (2005).

[4] N. I. Landy, S. Sajuyigbe, J. J. Mock, D. R. Smith and W. J. Padilla, Physical Review Letters **100**, 207402 (2008).

[5] N. Fang, H. Lee, C. Sun and X. Zhang, Science **308**, 534 (2005).

[6] D. Schurig, J. J. Mock, B. J. Justice, S. A. Cummer, J. B. Pendry, A. F. Starr and D. R. Smith, Science **314**, 977 (2006).

[7] X. L. Liu, T. Tyler, T. Starr, A. F. Starr, N. M. Jokerst and W. J. Padilla, Physical Review Letters **107**, 45901 (2011).

[8] Y. Wang, T. Sun, T. Paudel, Y. Zhang, Z. Ren and K. Kempa, Nano Letters **12**, 440 (2012).

[9] K. Iwaszczuk, A. C. Strikwerda, K. Fan, X. Zhang, R. D. Averitt and P. U. Jepsen, Optics Express **20**, 635 (2012).

[10] X. P. Shen, Y. Yang, T. Z. Zang, J. Q. Gu, J. G. Han, W. L. Zhang and T. J. Cui, Applied Physics Letters **101**, 154102 (2012).

[11] H. Tao, C. M. Bingham, A. C. Strikwerda, D. Pilon, D. Shrekenhamer, N. I. Landy, K, Fan, X. Zhang, W. J. Padilla and R. D. Averitt, Physical Review B **78**, 241103(R) (2008).

[12] D. Shrekenhamer, W. C. Chen and W. J. Padilla, Physical Review Letters **110**, 177403 (2013).

[13] Fei Fan, Wei Li, Wen-Hao Gu, Xiang-Hui Wang and Sheng-Jiang Chang, Photonics and Nanostructures-Fundamentals and Applications **11**, 48 (2013).

[14] Wei Li, Dengfeng Kuang, Fei Fan, Shengjiang Chang and Lie Lin, Applied Optics **51**, 7098 (2012).

[15] S. C. Howeels and L. A. Schlie, Applied Physics Letters **69**, 550 (1996).

[16] X. Y. Dai, Y. J. Xiang, S. C. Wen and H. Y. He, Journal of Applied Physics **109,** 053104 (2011).

[17] P. Halevi and F. Ramos-Mendieta, Physical Review Letters **85**, 1875 (2000).

[18] M. P. Hokmabadi, D. S. Wilbert, P. Kung and S. M. Kim, Optics Express **21**, 16455 (2013).

[19] M. A. Seo, H. R. Park, S. M. Koo, D. J. Park, J. H. Kang, O. K. Suwal, S. S. Choi, P. C. M. Planken, G. S. Park, N. K. Park, Q. H. Park and D. S. Kim, Nature Photonics **3**, 152 (2009).